ISTFA 2023: Proceedings of the 49th International
Symposium for Testing and Failure Analysis Conference
November 12—16, 2023, Phoenix, Arizona, USA
https://doi.org/10.31339/asm.cp.istfa2023p0309

Precise Final Thinning by Concentrated Ar Ion Beam Milling of Plan View TEM Specimens from Phase Change Memory Device Prepared in Xe Plasma FIB

C.S. Bonifacio, M.L. Ray and P.E. Fischione
E.A. Fischione Instruments, Inc., Export, PA USA

Y. Yu and M. Skowronski
Materials Science and Engineering, Carnegie Mellon University, Pittsburgh, PA USA

Abstract

Advanced memory technologies are in demand with phase change memory (PCM) devices as a forefront candidate. For successful characterization by transmission electron microscopy (TEM) for failure analysis and device development, an accurate and controllable thinning of TEM specimens is critical. In this work, TEM specimens from a GeTe-based PCM device at a partial SET state were prepared using a Xe plasma focused ion beam (pFIB) and polished to electron transparency using Ar ion beam milling. We will highlight the differences between Ga focused ion beam (FIB) and Xe pFIB TEM specimen preparation, the benefits of post-pFIB Ar ion beam milling, and show TEM results of the effects of partial SET programming of the GeTe PCM device.

Introduction

The preparation of transmission electron microscopy (TEM) specimens using a FIB system is a standard sample preparation approach because it allows site selectivity and can be accomplished quickly. Though a cross-sectional specimen configuration is typical, a plan view specimen configuration also can be prepared using a FIB system. There are many advantages to using plan view specimens, especially for device failure analysis: there is a higher probability of imaging a defect due to the larger field of view [1, 2] and the sample yields many repeating features on a single specimen [3] (unlike a small cross-section specimen). Combining results from both cross section and plan view analysis yields a full perspective of a defect in three dimensions. The choice of a plan view configuration, as opposed to a cross-section configuration, is relatively infrequent since plan view specimen preparation requires complicated sample manipulation and takes longer to accomplish. Because the plan view specimen is oriented parallel to the bulk sample surface, a large volume of material must be removed, especially beneath the region of interest (ROI).

Xe pFIB specimen preparation is ideal for preparing plan view TEM specimens due its large volume milling capabilities [4]. However, producing electron-transparent TEM specimens using a Xe pFIB system requires an adjustment of stage tilt and milling pattern placement; it deviates from the standard Ga FIB method due to the relatively large Xe beam and its wide beam tails [5]. Ga FIB preparation with post-FIB Ar ion beam milling of TEM specimens has been reported previously, but plan view TEM specimens prepared by a Xe pFIB system followed by concentrated Ar ion beam milling constitutes new work. Here, we employed post-FIB polishing by concentrated Ar ion beam milling on plan view TEM specimens prepared using a Xe pFIB system. Consequently, precise control of specimen thinning is achieved, which results in high quality specimens with pristine surfaces and large field of view for TEM characterization.

Discussion

For this study, GeTe-based, mushroom-type, phase change memory (PCM) devices were used to investigate the extent of phase transformation from amorphous to crystalline GeTe. PCM devices are of interest due to their non-volatility, high scalability, and compatibility with back-end-of-line processing [6]. GeTe-based mushroom cells were fabricated, electrically tested, and partially SET. The RESET state of PCM corresponds to an amorphous dome of the chalcogenide quenched in on top of the bottom electrode. The SET state is the fully crystallized functional layer and partial SET is an intermediate crystallization state. The transition from RESET to SET can occur purely by growth of the crystalline grains from the periphery toward the bottom electrode or by a combination of nucleation and growth. GeTe is thought to be growth-dominated material crystallizing primarily by growth. This characteristic, however, is device size-dependent and needs to be assessed by examination of real device structures. Realizing purely growth-driven crystallization can be potentially advantageous because it eliminates the stochastic nucleation step and makes it easier to control the partial SET processes. [7]. The GeTe-PCM crystallization process was imaged by the TEM cross-section technique. However, a quantitative assessment of the transformation rates can only be visualized using a plan view TEM specimen.

Post-pFIB polishing using concentrated Ar ion beam milling [PicoMill® TEM specimen preparation system, Fischione Instruments] on both cross-section and plan view TEM

specimens is an essential part of the preparation workflow. The GeTe layer in the PCM device is highly susceptible to ion beam damage, especially by Ga ions, and for this reason the Xe pFIB was used for bulk milling of the specimens. However, specimen thinning to electron transparency using the Xe pFIB is not trivial because of the large Xe beam diameters and the prominent beam tails of the Xe beam make fine-scale milling complex [5]. Subsequently, controlled specimen thinning of the GeTe-based PCM device was achieved using the PicoMill system's concentrated Ar ion beam. Furthermore, the electron imaging capability of the PicoMill system was valuable for visualization of the Pt protective layer removal in the plan view specimens and electron transparency for both plan view and cross-section specimens.

GeTe-based mushroom cells were fabricated, electrically tested, and left in the partial SET state. Cross-section and plan view TEM specimens from the GeTe-based PCM were prepared in a Xe pFIB system. Post-FIB Ar ion beam milling was performed in the PicoMill system using the high-tilt method [8-10], which resulted in controlled and reproducible specimen thinning. Various TEM techniques were performed to identify the amorphous and polycrystalline areas on the GeTe layer of the PCM device.

Specimen preparation using the pFIB

A Helios dual beam pFIB [Thermo Fisher Scientific] was used for preparation of cross-section and plan view TEM specimens. In this system, the electron source and Xe ion source traverse at 52°. Cross-section and plan view TEM specimens were successfully prepared using the pFIB milling adjustments suggested by Vitale and Sugar [5]. The plan view pFIB preparation will be discussed in more detail. However, for both specimen types, the final polishing steps are the same and will be highlighted in this section.

Figure 1a is a top view, scanning electron microscope (SEM) image of the mushroom PCM device. The active device area corresponds to a small square in the center of the image with and even smaller bottom electrode (not visible in the image) located in the center of the square. The area marked by the red rectangle corresponds to the shape of the cross-section TEM specimen. The schematic of the device (inset of Figure 1a) provided information for which layers to remove during the plan view specimen preparation.

It is imperative to deposit a protective Pt layer on the device (labelled area in Figure 1a) because the GeTe is susceptible to ion beam damage. The 1 µm thick Pt layer was deposited using the electron beam (2 kV and 1.4 nA) and by Xe ion beam (8 kV and 3.7 nA). Figures 1b-f are schematic diagrams of the plan view preparation with the steps summarized in Table 1. This process is based on a modified plan view Ga FIB preparation [10]. In this case, the total milling time was reduced from ~3 hours using the Ga FIB to ~1.5 hours with Xe pFIB due to higher milling rates in the pFIB.

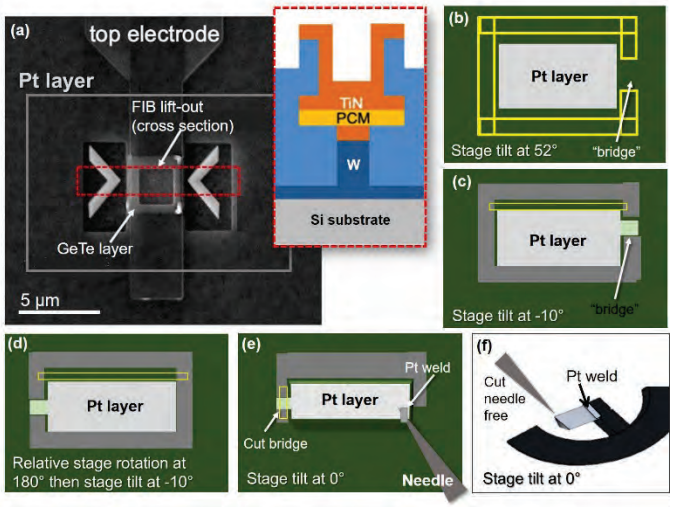

*Figure 1: Scanning electron microscopy top view image (**a**) of the GeTe-based PCM device with the position of the GeTe layer identified. Inset of **a** shows a schematic in cross section across GeTe layer. Plan view pFIB specimen preparation steps are shown as illustrations (**b-f**) from the ion beam perspective with yellow boxes as milling patterns used during FIB milling.*

Table 1: Plan view specimen preparation parameters performed at 30 kV voltage in the pFIB.

Step	Task	Stage tilt	Stage rotation	Pattern type	Ion beam current
a	Deposit Pt on the ROI (15 µm wide x 10 µm) height	0 and 52°	0°	Rectangle	2 kV, 1.4 nA Ebeam 8 kV, 3.7 nA Ibeam
b	Cut C-shaped channel around the ROI that creates a "bridge"	52°	0°	Regular cross section with depth or z ≥ 5 µm	15 nA, 6.7 nA
c	Make a wedge on the long side of the specimen	-10.4°	0°	Cleaning cross section with depth or z =10 µm	6.7 nA, 1.8 nA
d	Make a wedge on the long side of the specimen	-10.4°	180° from Step c position (Figure 1d)	Cleaning cross section with depth or z = 10 µm	6.7 nA, 1.8 nA
e	Mount the specimen chunk to the needle with Pt; cut the specimen free from the bulk	0°	Stage rotation as in Step d (Figure 1e)	Rectangle	0.23 nA

Step	Task	Stage tilt	Stage rotation	Pattern type	Ion beam current
f	Transfer and mount the specimen to the grid with Pt; cut the needle free	0°	Stage rotation as in Step e (Figure 1f)	Rectangle	0.23 nA

Once the chunk was lifted out and welded onto the grid, the pFIB polishing steps (summarized in Table 2) for pre-thinning the TEM specimen were performed. The polishing steps in Table 2 were used for both cross-section and plan view specimens. However, for the plan view specimen, most of the milling was performed at the back side of the specimen (silicon substrate) and significantly less at the front side covered by the Pt layer. The back of the bulk plan view TEM specimen after FIB lift-out is wedge-shaped (Figure 2a).

It should be noted that specimen thinning using the Xe pFIB was significantly different than using the Ga FIB. The placement of the milling box was crucial in successfully milling the GeTe-based PCM specimen using the pFIB. The milling box is placed away from the edge of the specimen (rectangular box in Figure 2a) during pFIB milling. For the same ion energy of 30 kV, the Xe beam in the pFIB is wide at low currents and sharp and narrow at higher currents. The full width half maximum (FWHM) of cross sections of Xe beam burns on Si were 0.48 µm at 300 pA and 1.87 µm at 60 nA [5]. The milling box was placed further away from the edge of the specimen as the milling beam current was decreased to prevent over milling the top of specimen. Thinning of the specimen still occurred due to the beam tails, which extend beyond the bounds of the milling pattern [5]. In terms of specimen tilt, a larger tilt adjustment (gradual increase to 57°) was necessary because the GeTe layer and ROI was in the center of the specimen. Also, significant specimen tilt of 57º was used at 5 kV to polish the specimen to remove the sample surface damaged by the Xe beam. Because of the stage tilt limitation in the pFIB, the specimen was rotated 180º to access the front of the specimen for 5 kV milling.

Table 2: pFIB specimen thinning parameters performed at 30 kV and 5 kV FIB voltages.

Orientation	Stage tilt	Pattern type	Energy and ion beam current
Back and front side pFIB thinning	52-57°	Regular cross-section with depth or Z < 2 µm	30 kV at: – 230 pA – 24 pA
Back and front side pFIB polishing	57°	Rectangle	5 kV at 12 pA

Figure 2b and Figure 2c show the front and back sides of the plan view TEM specimen from the GeTe device after Xe pFIB milling. Based on the image contrast, the specimen thickness varies with the bottom part of the plan view TEM specimen being thinnest (Figure 2b). Also, one can notice the curtaining artifacts on the back side of the specimen (Figure 2c).

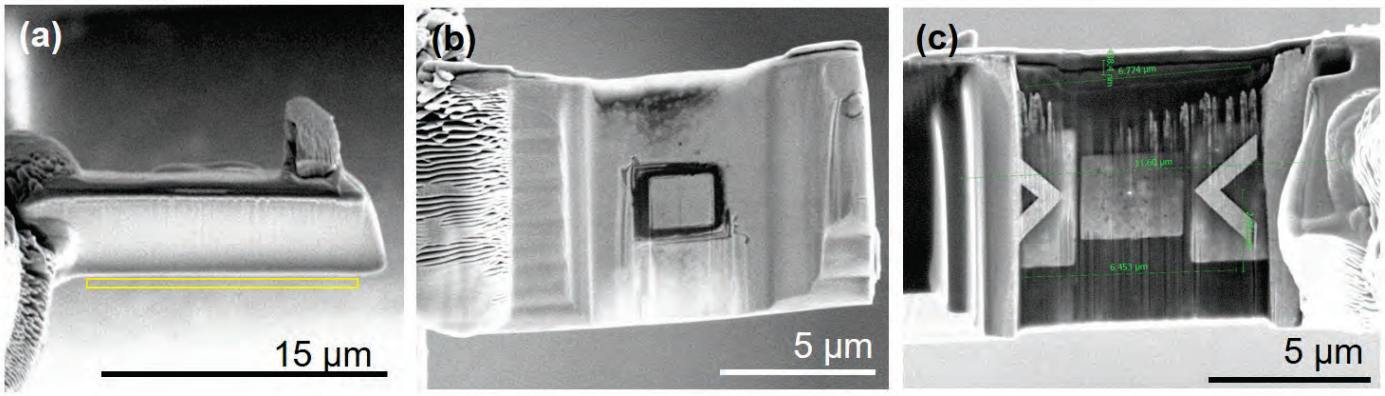

*Figure 2: Scanning electron microscopy image of the GeTe-based PCM device after bulk milling and lift-out to the grid (**a**) and after thinning steps at 30 kV and 5 kV of the front (**b**) and back (**c**) sides of the plan view specimen. Rectangular box in **a** represents the position of the milling box during milling in the pFIB, which is away from the specimen edge.*

Post-FIB milling using a concentrated Ar ion beam

The Ar ion beam milling system, which has a 600 nm diameter Ar ion beam, was used to thin the FIB specimens to electron transparency. The system includes a LaB_6 electron source and electron detectors – a secondary electron detector (SED) and a scanning transmission electron microscope (STEM) – that provide in situ imaging capability during ion milling. The grid with the FIB specimen was mounted on a specimen holder that is compatible with both the Ar ion beam milling system and the TEM. The grid was mounted with the fingers of the grid pointing toward the bottom (Figure 3). Controlled, large area Ar ion beam milling of the specimens [8-10] was achieved by high-tilt Ar milling with the Ar beam hitting the bottom part of the specimen first. By tilting the specimen at a 15°, the ROI, which is at the center of the specimen, is exposed as depicted in Figure 3. A user-defined milling box with size of 10 x 3 µm (width x height) was placed near the middle of the specimen; the small, concentrated beam of argon ions moved in a raster pattern within the box. Decreasing energies were employed – 900 eV for the removal of the Pt layer to 700 eV for specimen thinning.

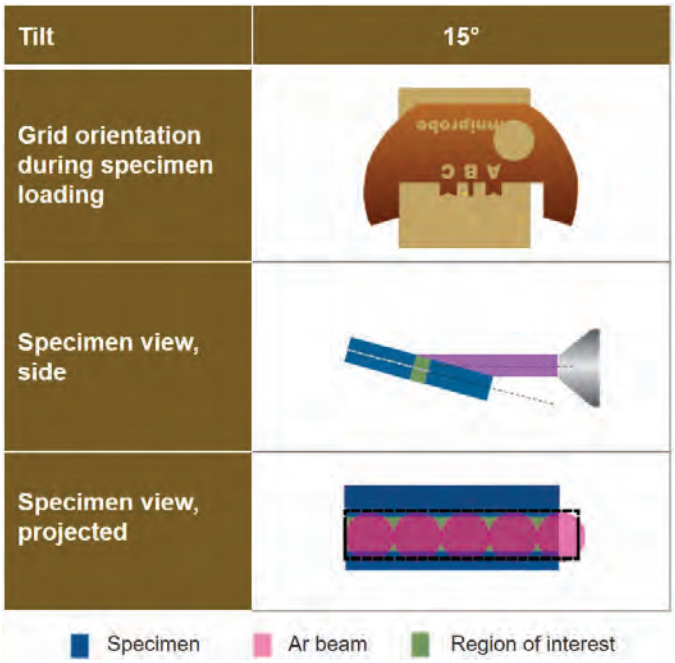

Figure 3: Parameters for high-tilt backside concentrated Ar ion beam milling showing grid orientation, specimen tilt of 15° and the relationship between Ar beam and ROI on the specimen. Side view and projected view of the specimen with respect to the Ar beam show the increased exposure of the ROI to the Ar beam at 15°.

Final thinning of both cross-section and plan view TEM specimens was performed using Ar ion beam milling. The post-pFIB milling step not only precisely thinned the specimen to electron transparency, but also prevented the exposure of the GeTe layer to the potentially damaging ion beams during pFIB preparation. Specifically to the plan view specimen, removal of the layers in the front and back side of the specimen to target the GeTe layer was performed. Pt layer and the TiN layers in the front and Si substrate and W contact in the back (inset of Figure 1a) were removed by using the Ar ion beam milling system. It was important to stop milling on the PCM layer to characterize the affected region during the partial SET state operation, which can easily be milled off.

Figure 4 shows electron transparency of the plan view specimen after Ar ion beam milling. Specimen thinning was achieved leaving behind the GeTe layer with part of the W contact intact, which is where the affected region after partial SET process is expected. The front side of the specimen (Figure 4a) showed partially removed TiN and Pt layers exposing the fiducial marks on the ROI. At the back side of the specimen (Figure 4b), most of the Si substrate was removed, leaving only part of the W contact. Furthermore, the curtaining artifacts previously observed after pFIB milling (Figure 2c) were removed by Ar ion beam milling (Figure 4b).

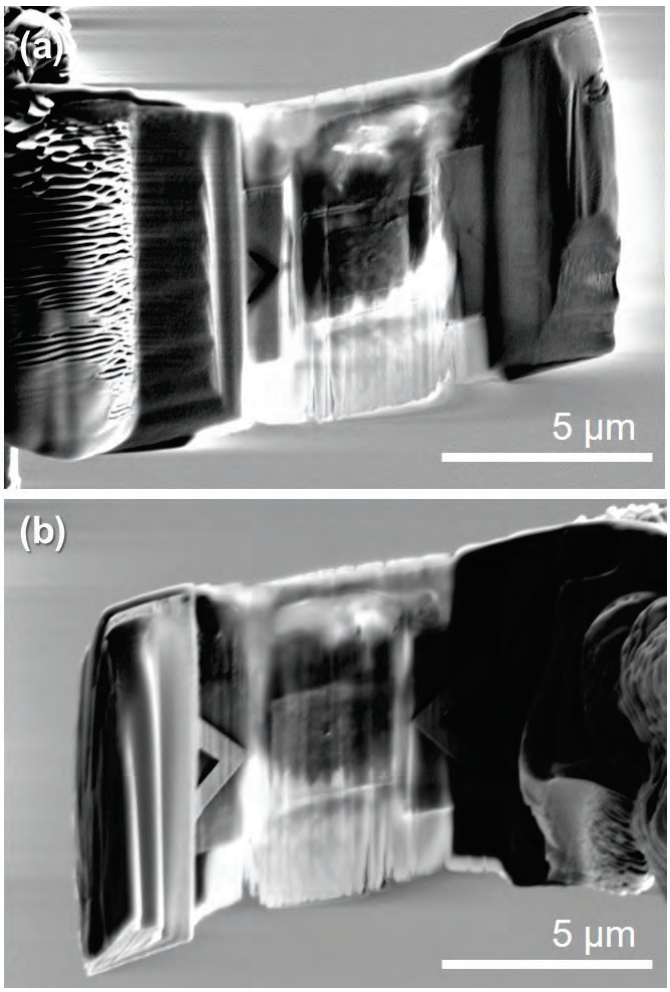

*Figure 4: Scanning electron microscopy image of the GeTe-based PCM device after Xe pFIB milling, followed by concentrated Ar ion beam milling of the front side (**a**) and back side (**b**) of the plan view TEM specimen.*

Characterization of partial SET process in the PCM device using the cross-section TEM specimens

Phase transformations and elemental distributions in the GeTe layer as a result of the applied electrical operations were identified using TEM techniques. Specifically, we were interested in imaging the intermediate states to understand the crystallization mechanism in the transition from the amorphous RESET state back to crystalline SET state. This was achieved by leaving the device in partial SET state; the PCM layer still contains a partially crystallized amorphous dome on top of the bottom electrode. Various TEM techniques were performed: bright field high resolution TEM imaging and precession electron diffraction (PED) to differentiate the amorphous and crystalline areas.

The initial morphology and the changes at partial SET state of the GeTe layer of the PCM device were determined by analyzing the cross-section TEM specimens. Before pFIB preparation and subsequent Ar ion beam milling, the PCM device was left in a partial SET state by applying a rectangular RESET pulse (8 V and 200 ns), followed by a partial SET pulse (1.8 V and 50 ns). The cross-section TEM specimen prepared in the pFIB after device fabrication and after programming to a partial SET state were compared (Figure 5). The low magnification TEM image (Figure 5a) shows the GeTe PCM layer between the TiN top electrode and W bottom electrode of the as fabricated device. The as fabricated PCM layer is polycrystalline with grains 100 nm in size (Figure 5b).

The partial SET specimen in Figure 5c prepared by pFIB milling and post pFIB Ar ion beam milling (Figure 5c) was of high quality and suitable for high resolution TEM imaging; the crystalline and amorphous areas are easily differentiated. The initial polycrystalline GeTe layer has a 160 nm wide affected area (marked with dashed line, Figure 5c) off-center from the W electrode at the partial SET state. This affected region is composed of a crystalline area over a 107 nm wide amorphous dome. Using PED, area I (I in Figure 5d) was found to be a mixture of crystalline and amorphous areas based on the distinct diffraction intensities and diffused ring near the center. Adjacent to area I was area II with diffused ring of diffraction intensity (II in Figure 5d) corresponding to amorphous GeTe. The crystallization process was identified as purely growth-based; crystallization initiated from the crystalline-amorphous boundary moving towards the bottom electrode [7].

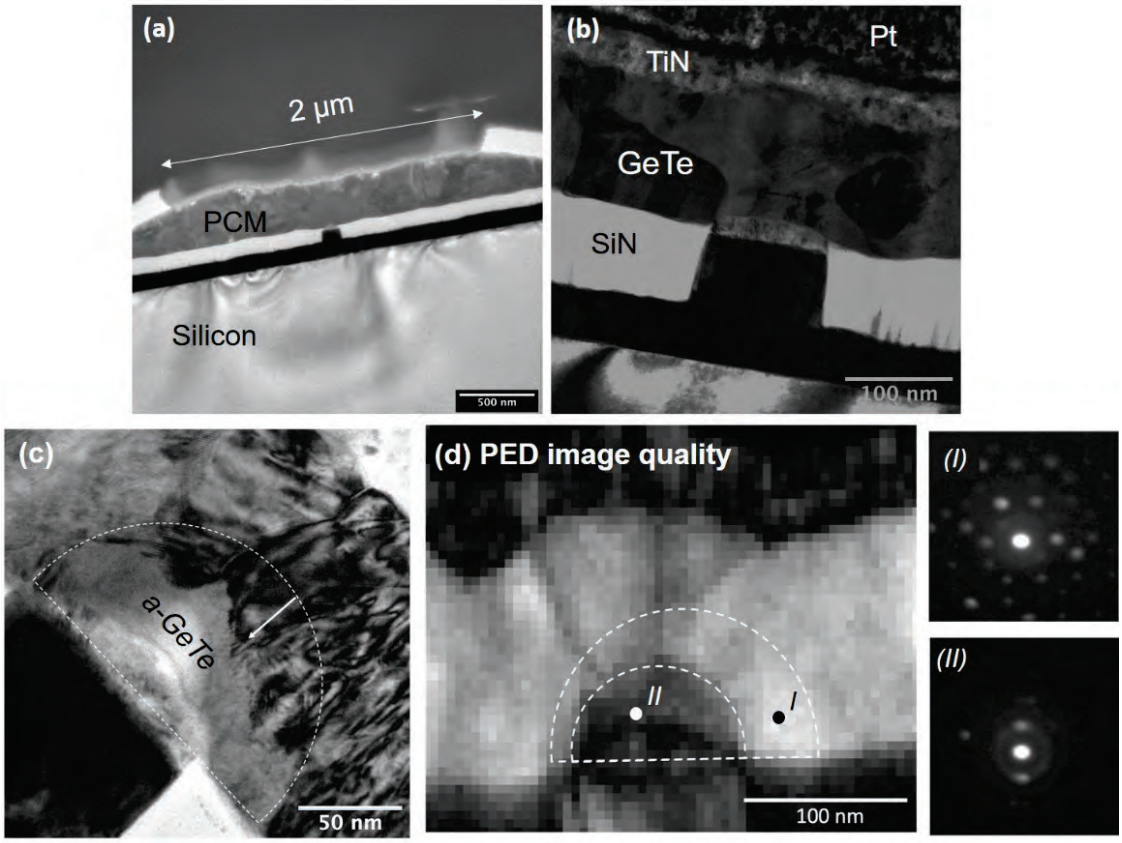

*Figure 5: TEM bright field images of cross-section specimens from the GeTe-based, mushroom-type, phase change memory (PCM) device (**a, b**) as fabricated and (**c**) after partial SET operation prepared using the Xe pFIB, followed by concentrated Ar ion beam milling. The high resolution (**b, c**) TEM images display the change in the initial (**b**) polycrystalline GeTe layer that forms an area with a mixture of (arrow in **c**) crystalline and (a-GeTe in **c**) amorphous areas just above the W bottom electrode. (**d**) Precession electron diffraction (PED) confirmed areas with mixed crystalline and amorphous region (I in **d**) and fully amorphous region (II in d) corresponding to the a-GeTe in **c**.*

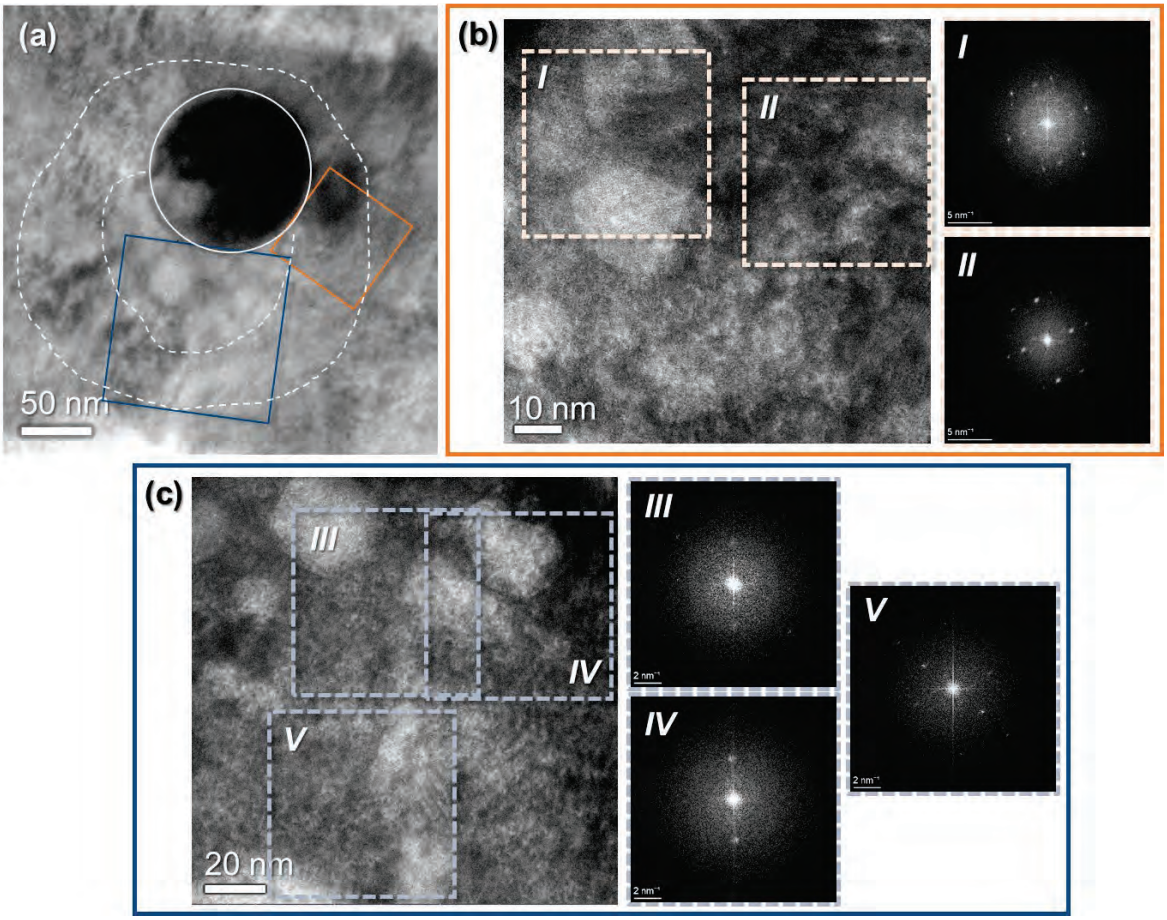

*Figure 6: TEM bright field image of the plan view specimen from the GeTe-based phase change memory (PCM) device at partial SET state (**a**) labelled with the areas (**b,c**) from which fast Fourier transforms (FFTs) were acquired. FFTs from areas (**b**) and (**c**) show areas with a strong diffused ring of intensities, amorphous GeTe (Areas III, IV) and areas with combination of distinct diffraction intensities and diffused ring of intensities, partially crystallized GeTe (Areas I, II and V).*

Extent of affected area by partial SET process using the plan view TEM specimen

The plan view TEM specimens after Ar ion beam milling were electron-transparent and suitable for high resolution imaging. High resolution TEM imaging and high-angle annular dark field scanning TEM (HAADF-STEM) with energy dispersive X-ray spectroscopy (EDS) were performed to determine the phase changes and elemental segregations on the GeTe layer. The affected region with the amorphous and crystalline areas initially observed in the cross-section specimen was identified on the plan view specimen.

The acquired HRTEM images were analyzed by fast Fourier transform (FFT) analysis to identify the crystalline and amorphous GeTe areas. Figure 6a shows the functional layer around the W bottom electrode from which HRTEM images were acquired for FFT analysis. Two areas, areas in orange (Figure 6b) and in blue (Figure 6c), were examined. The FFTs from the HRTEM images display distinct diffraction intensities and diffused halo of diffraction intensities related to the crystalline and amorphous phase, respectively. The FFT from Area 1 and II (Figure 6b) show well-defined diffraction intensities with faint diffused ring of intensity similar to the PED results from the cross-section specimen, I in Figure 5d, identified as partially crystallized GeTe. In contrast, the area in blue (Figure 6a) was mostly amorphous GeTe with III and IV (Figure 6c) showing strong diffused ring intensities with the V (Figure 6c) toward the edge similar to II (Figure 6b), which is partially crystallized GeTe. Based on these results, the affected region on the plan view specimen was defined in Figure 6a — the inner area near the W bottom electrode as amorphous GeTe and the outer areas as partially crystallized GeTe. This affected region (Figure 6a) was measured as 237 nm in diameter; within this area is a 130 nm diameter amorphous region. The amorphous GeTe area was off-center from the W bottom electrode, which was similar to the cross-section specimen results.

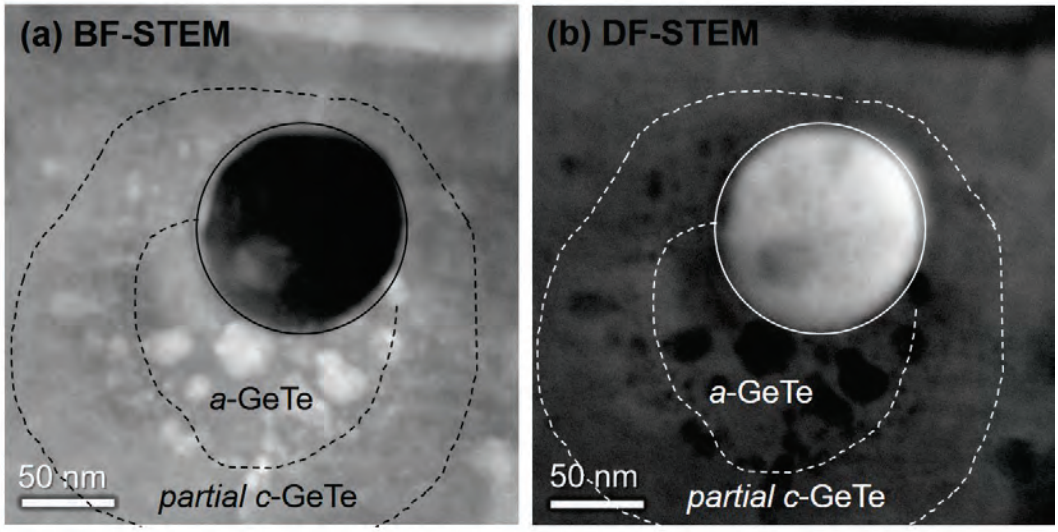

*Figure 7. Bright field STEM (**a**) and dark field STEM (**b**)images of the plan view specimen from the GeTe-based phase change memory (PCM) device in Figure 6 after partial SET operation marked with the affected region composed of amorphous GeTe (a-GeTe) and partially crystallized GeTe (partial c-GeTe).*

With the same applied partial SET programming, the extent of the affected region was established to be larger than what was observed from the cross-section TEM specimen: 237 nm in diameter (Figure 6a) compared to 160 nm width (Figure 5c). Such results demonstrate the advantage of preparing a plan view specimen over cross-section specimens; it provides a large field of view that captures variation in the device.

The same areas of the partially crystallized GeTe and amorphous GeTe were identified and labelled (*partial c-GeTe and a-GeTe* in Figure 7) on the STEM images. The STEM images, bright field (BF-STEM) and dark field (DF-STEM) images (Figures 7a-b) acquired simultaneously revealed areas of high intensity contrast in the BF-STEM corresponding to dark intensity contrast in the DF-STEM image. For HAADF-STEM imaging, these areas of lower Z-contrast are attributed to lower local density or voids. These voids were located mostly in the amorphous GeTe and were verified to be inherent to the device as a result of the electrical programming, i.e., they were not caused by the specimen preparation. Previous work [11] has shown similar voids on a GeSbTe-based PCM device, which were attributed to moderately large voltage and very long durations at constant-amplitude pulse.

EDS elemental mapping revealed the distribution of Ge and Te in the PCM device after RESET and partial SET biasing. Figure 8a is a combined EDS map for Ge and Te with individual maps in Figure 8b and Figure 8c, respectively. The area marked with circle represents the position of the W bottom electrode. The non-uniform Ge and Te distributions near the electrode matches with the affected region identified in the HRTEM (Figure 6) and HAADF-STEM (Figure 7) results. These regions were marked on the HAADF-STEM image in Figure 8d. The line profile (Figure 8e) acquired across the affected region from the W electrode exactly showed the elemental distribution in the affected region. From Figure 8e, the amorphous GeTe area was found to have high distribution of Ge, while the partially crystallized GeTe as Te-rich. The void with low intensity contrast on the amorphous GeTe, positioned between 57.5 nm to 85 nm, was found to be Te-rich (Figure 8e). It can be concluded that during partial SET process, Ge is driven towards the W bottom electrode and leaves behind a Te-rich layer. During the GeTe segregation, the Ge-rich areas become amorphous; current can be confined and subsequently voids are created [11].

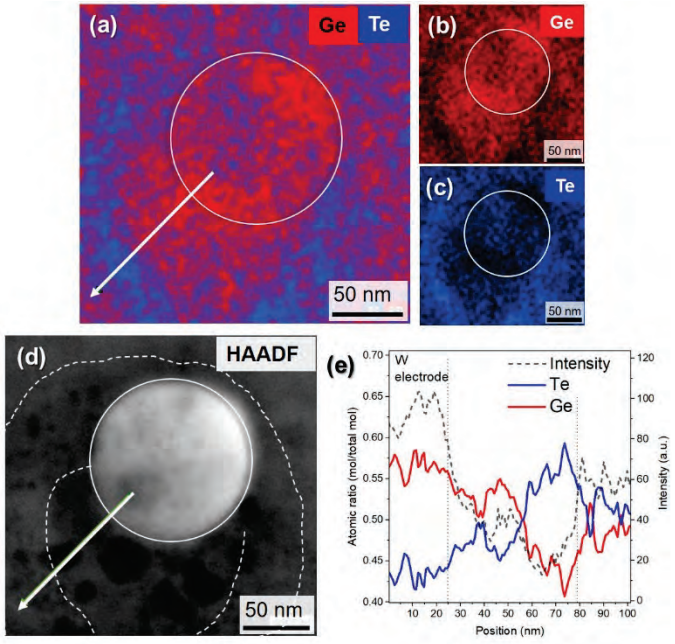

*Figure 8. Energy dispersive X-ray spectroscopy (EDS) maps showing combined GeTe (**a**) and individual EDS map of Ge (**b**) and Te (**c**). The corresponding elemental distribution and HAADF-STEM intensity in (**d**) from which the EDS line profile was acquired are plotted in (**e**).*

The overall description of the crystallization by pure growth can be deduced based on electron microscopy results from the plan view TEM specimen. The crystallization front moves from the crystallization region toward the W bottom electrode, which is similar to results from the cross-section TEM specimens [7]. For the plan view specimen, the trace of crystallization front was initiated from the Te-rich Areas I, II, and V (Figure 6 and Figure 8a,c) with presence of both distinct diffraction intensities and diffused ring diffraction intensities to the partially crystallized GeTe Areas III and IV (Figure 6) with diffused ring diffraction intensities and finally the amorphous GeTe where the voids formed. This partially crystallized GeTe can be completely crystallized during the SET operation by a gradual sweep down of the voltage across the PCM device [7]. Most importantly, the segregation of Ge and Te detected from the EDS maps along with the void formation correlated to results in [11].

Conclusions

Plan view TEM specimen preparation of the GeTe-based PCM device using the Xe pFIB with post-FIB Ar ion beam milling was established. As a result, the phase transformation and elemental distribution within the GeTe layer in the partial SET state of the device were identified by TEM techniques. The area affected by the partial SET pulse was identified as Te-rich, partially crystallized GeTe, and a Ge-rich, amorphous GeTe with voids found close to the W bottom electrode. Most importantly, post-pFIB Ar ion beam milling was an important specimen preparation step to achieve electron-transparent specimens by precise control of specimen thinning of both cross-section and plan view TEM specimens. Specimens prepared by Xe pFIB can be thicker, and then further polished using Ar ion beam milling. The result is high quality specimens with large field of views and pristine surfaces for TEM characterization.

References

[1] Zhu, J., Du, A. Y., Liu, B. H., Er, E., Zhao, S. P., & Lam, J. (2014). Tri-Directional TEM Failure Analysis on Sample Prepared by In-Situ Lift-Out FIB and Flipstage. *International Symposium for Testing and Failure Analysis*. https://doi.org/10.31399/asm.cp.istfa2014p0480

[2] Meyer, T., Westphal, T., Kressdorf, B., Ross, U., Jooss, C., & Seibt, M. (2021). Site-specific plan-view TEM lamella preparation of pristine surfaces with a large field of view. *Ultramicroscopy*, *228*, 113320. https://doi.org/10.1016/j.ultramic.2021.113320

[3] Stevie, F. A., Irwin, R. B., Shofner, T. L., Brown, S. R., Drown, J. L., & Giannuzzi, L. A. (1998). Plan view TEM sample preparation using the focused ion beam lift-out technique. *Characterization and Metrology for ULSI Technology*. https://doi.org/10.1063/1.56881

[4] Zhong, X., Wade, C. A., Withers, P. J., Zhou, X., Cai, C., Haigh, S. J., & Burke, M. N. (2021). Comparing Xe^+ pFIB and Ga^+ FIB for TEM sample preparation of Al alloys: Minimising FIB - induced artefacts. *Journal of Microscopy*, *282*(2), 101-112. https://doi.org/10.1111/jmi.12983

[5] Vitale, S., & Sugar, J. D. (2022). Using Xe Plasma FIB for High-Quality TEM Sample Preparation. *Microscopy and Microanalysis*, *28*(3), 646–658. https://doi.org/10.1017/s1431927622000344

[6] Burr, G. W., BrightSky, M. J., Sebastian, A., Cheng, H., Wu, J., Kim, S., Sosa, N. E., Papandreou, N., Lung, H., Pozidis, H., Eleftheriou, E., & Lam, C. H. (2016). Recent Progress in Phase-Change Memory Technology. *IEEE Journal on Emerging and Selected Topics in Circuits and Systems*, *6*(2), 146–162. https://doi.org/10.1109/jetcas.2016.2547718Zhu, J., Du, A. Y., Liu, B. H., Er, E., Zhao, S. P., & Lam, J. (2014). Tri-Directional TEM Failure Analysis on Sample Prepared by In-Situ Lift-Out FIB and Flipstage. *International Symposium for Testing and Failure Analysis*. https://doi.org/10.31399/asm.cp.istfa2014p0480

[7] Yu, Y., & Skowronski, M. (2023). Growth dominated crystallization of GeTe mushroom cells during partial SET operation. *Journal of Applied Physics*, *133*(4), 044501. https://doi.org/10.1063/5.0129023

[8] C. S. Bonifacio et al., "Cutting-edge sample preparation from FIB to Ar concentrated ion beam milling of advanced semiconductor devices," *Proc 46th Int'l Symp for Testing and Failure Analysis*, event cancelled, November 2020, p 133-140. doi:10.31399/asm.cp.istfa2020p0133

[9] C. Bonifacio et al., "High throughput and multiple length scale sample preparation for characterization and failure analysis of advanced semiconductor devices," *Proc 45th Int'l Symp for Testing and Failure Analysis*, Portland, OR, November 2019, p 295-301. doi:10.31399/asm.cp.istfa2019p0295

[10] C.S. Bonifacio, et al., "Large Field of View and Artifact-Free Plan View TEM Specimen Preparation by Post-FIB Ar Milling." Proceedings of the *ISTFA 2022. ISTFA 2022: Conference Proceedings from the 48th International Symposium for Testing and Failure Analysis*. Pasadena, California, USA. October 30–November 3, 2022. (pp. 181-189).

[11] Padilla, A., Burr, G. W., Rettner, C. T., Topuria, T., Rice, P. M., Jackson, B. L., Virwani, K., Kellock, A. J., Dupouy, D. G., Debunne, A., Shelby, R. M., Gopalakrishnan, K., Shenoy, R. S., & Kurdi, B. N. (2011b). Voltage polarity effects in $Ge_2Sb_2Te_5$-based phase change memory devices. *Journal of Applied Physics*, *110*(5), 054501. https://doi.org/10.1063/1.3626047